Journal of Molecular Spectroscopy **213,** 170–178 (2002)
doi:10.1006/jmsp.2002.8565

Fourier Transform Emission Spectroscopy of the $F^2\Sigma^+$–$X^2\Sigma^+$ System of RuN

R. S. Ram and P. F. Bernath[1]

Department of Chemistry, University of Arizona, Tucson, Arizona 85721

Received December 17, 2001; in revised form March 11, 2002

Emission spectra of RuN have been recorded at high resolution in the region 12 000–35 000 cm^{-1} using a Fourier transform spectrometer. The molecules were excited in a ruthenium hollow cathode lamp in the presence of about 2.5 Torr of Ne and 5 m Torr of N_2. New bands with origins near 17 758.1, 18 866.4, 19 800.4 and 20 721.5 cm^{-1} have been assigned as the 0–1, 0–0, 1–0, and 2–0 bands of a new $^2\Sigma^+$–$^2\Sigma^+$system with the lower state as the ground state. This transition has been labeled as $F^2\Sigma^+$–$X^2\Sigma^+$, with the $F^2\Sigma^+$ state arising from the $1\sigma^2 2\sigma^2 1\pi^4 1\delta^4 4\sigma^1$ configuration. A rotational analysis of these bands has been carried out and spectroscopic constants have been extracted. The principal equilibrium constants for the ground state of RuN are $\Delta G(1/2)'' = 1108.3235(22)$ cm^{-1}, $B_e'' = 0.5545023(42)$ cm^{-1}, $\alpha_e'' = 0.0034468(57)$ cm^{-1}, $r_e'' = 1.5714269(60)$ Å, while the equilibrium constants for the excited state are $\omega_e' = 946.8471(40)$ cm^{-1}, $\omega_e x_e' = 6.4229(14)$ cm^{-1}, $B_e' = 0.50085(21)$ cm^{-1}, $\alpha_e' = 0.00375(10)$ cm^{-1}, $r_e' = 1.65345(34)$ Å. This transition is analogous to the $E^2\Sigma^+$–$X^2\Sigma^+$system of RhC (W. J. Balfour *et al.*, *J. Mol. Spectrosc.* **198,** 393 (1999)).

INTRODUCTION

Transition-metal-containing diatomics provide models to help in our understanding of bonding and reactivity in transition metal systems (*1*). These species are also of chemical importance, particularly in catalysis (*2–4*). Because of the high cosmic abundance of transition metal elements in stars, some diatomic species are also of astrophysical importance and several diatomic oxide and hydride molecules have been identified in the atmospheres of cool M- and S-type stars (*5–9*). Although transition metal nitrides have not been identified in the stellar atmospheres, precise spectroscopic data are necessary for a meaningful search in complex stellar spectra. We have initiated a program to assemble high-resolution data for transition metal nitrides to assist in the search of these species in stellar atmospheres.

In recent years, a number of transition metal nitride molecules have been observed in the gas phase and their electronic spectra have been characterized at high resolution (*10*). For the group 8 transition metal family, in particular, high-resolution spectroscopic data are now available for FeN (*11*), RuN (*12*), and OsN (*13*). In an extensive study, Aiuchi and Shibuya (*11*) generated FeN in the reaction of laser-ablated Fe atoms with NH_3 using a supersonic jet expansion source and analyzed a number of bands. The ground state of FeN has been identified as the $\Omega = 5/2$ spin component of a $^2\Delta_i$ state (*11*). RuN (*12*) and OsN (*13*) have also been investigated recently at high resolution and ground states of $^2\Sigma^+$ and $^2\Delta_i$ symmetry (respectively) have been established. *Ab initio* calculations for FeN (*14, 15*), RuN (*12*), and OsN (*13*) molecules have also been carried out recently and the experimental assignments are supported by these calculations.

The reaction of laser-ablated ruthenium and osmium atoms with nitrogen has been studied by Citra and Andrews (*16*) and products were isolated in solid argon and nitrogen matrices at cryogenic temperatures. In addition to dinitrogen complexes, the diatomic RuN and OsN molecules were observed and classified by their matrix infrared spectra. The bonding properties of the 3*d*-, 4*d*-, and 5*d*-transition metal nitride and carbide solids have been studied by Häglund *et al.* (*17*).

The first observation of RuN was reported recently when the $C^2\Pi$–$X^2\Sigma^+$ transition was observed in the near infrared (*12*). This assignment was supported by *ab initio* calculations of the spectroscopic properties of the low-lying electronic states (*12*). In the present work we have recorded the emission spectrum of RuN in the 12 000–35 000 cm^{-1} region using a Fourier transform spectrometer and report the observation of a new $^2\Sigma^+$–$^2\Sigma^+$ transition with a 0–0 band near 18 866.4 cm^{-1}. Although the excited $^2\Sigma^+$ state was not calculated in our previous *ab initio* study (*12*), the present assignments are consistent with, and supported by, the results available for the isovalent RhC molecule (*18–21*). In this paper we report the rotational analysis of the 0–1, 0–0, 1–0, and 2–0 bands of the new transition.

EXPERIMENTAL DETAILS

The details of the experimental setup used in this experiment have been provided in our previous publication (*12*). In short, the molecules were produced in a Ru hollow cathode lamp in

[1] Also at Department of Chemistry, University of Waterloo, Waterloo, Ontario, Canada N2L 3G1.

0022-2852/02 $35.00

the presence of 2.5 Torr of Ne and about 5 m Torr of N_2 and the lamp was operated at 310 V and 235 mA current. The spectra were recorded with the 1-m Fourier transform spectrometer associated with the McMath–Pierce Telescope of the National Solar Observatory at Kitt Peak.

The spectra in the region 12 000–35 000 cm^{-1} were recorded in two parts. The region 12 000–24 000 region was recorded using a visible beam splitter and super blue Si-diode detectors by coadding 15 scans in about 2 h of integration at a resolution of 0.03 cm^{-1}. Although the four new bands observed in the region 17 500–22 000 cm^{-1} were clearly present in this spectrum, they were too weak for a rotational analysis. The region, 17 000–35 000 cm^{-1} was, therefore, recorded again in another experiment using a UV beam splitter, $CuSO_4$ filters, and midrange Si-diode detectors. This time 38 scans were co-added in about 7 h of integration at a resolution of 0.02 cm^{-1}. The visible transition is found to be much weaker in intensity than the near infrared one observed previously (*12*). In spite of such a long integration, the spectra were observed with only moderate intensity but were suitable for rotational analysis. In addition to the RuN bands, the observed spectra also contained Ru and Ne atomic lines as well as the N_2 and N_2^+ molecular lines. The emitter of the new bands was identified from the characteristic $^{100}Ru/^{102}Ru/^{104}Ru$ (ratio 2 : 5 : 3) isotope splitting and the close similarity of the lower state vibrational intervals of the new transition with the ground state vibrational intervals observed for the $C^2\Pi$–$X^2\Sigma^+$ transition of RuN (*12*). The new RuN bands were relatively free from overlapping from N_2 bands although the 0–0 band was partly overlapped by a N_2^+ band at 18 889 cm^{-1} which was easily distinguished from RuN by its larger line spacing.

The line positions were extracted from the observed spectra using a data reduction program called PC-DECOMP developed by J. Brault. The peak positions were determined by fitting a Voigt lineshape function to each spectral feature. The branches in the different bands were sorted using a color Loomis–Wood program running on a PC computer. The spectra were calibrated using the measurements of Ne atomic lines made by Palmer and Engleman (*22*). The RuN lines in the stronger bands appear with a maximum signal-to-noise ratio of about 8 and have a typical linewidth of about 0.04 cm^{-1}. The absolute accuracy of the wavenumber scale is expected to be on the order of ± 0.003 cm^{-1}. However, the isotopic lines in the 0–0 band are only partly resolved and in the other bands there is frequent overlapping from the lines of the minor isotopomers, so the precision of the measurements for the weaker and overlapped lines is limited to ± 0.005 cm^{-1}.

OBSERVATION AND ANALYSIS

The new RuN bands are located in the 17 500–22 000 cm^{-1} region. The four bands with origins near 17 758.1, 18 866.4, 19 800.4, and 20 721.5 cm^{-1} have been assigned as the 0–1, 0–0, 1–0, and 2–0 bands, respectively, of a new $^2\Sigma^+$–$^2\Sigma^+$ transition of RuN. The rotational analysis of the 0–0, 1–0, and 2–0 bands was carried out using the spectrum recorded in the second experiment. The 0–1 band in this spectrum was weakest in intensity, partly because it lies near the edge of the filters. Therefore, the analysis of this band was performed using the spectrum recorded in the first experiment described earlier, in spite of its weaker intensity. The spectrum of each band of the new transition consists of two *R* and two *P* branches with similar intensity, along with their isotopic companions. Ruthenium has three major isotopes with zero nuclear spin, ^{100}Ru (12.7%), ^{102}Ru (31.6%), and ^{104}Ru (18.7%) but our analysis concentrated only on the most abundant isotopomer ^{102}RuN. The lines of the minor isotopomers were also observed in the spectra of stronger bands. Our color Loomis–Wood program was very helpful in identifying the rotational lines of minor isotopomers even in the weaker bands. The isotopic lines in the 0–0 band were only partly resolved at lower *J*, although the high-*J* isotopic lines were completely resolved. In the 0–1, 1–0, and 2–0 bands the lines for all three isotopomers were well separated. A part of the 1–0 band is illustrated in Fig. 1, where lines belonging only to the major isotopomer ^{102}RuN have been marked for the sake of clarity.

The rotational analysis of the new bands indicated that the new transition has its lower state in common with the lower state of the $C^2\Pi$–$X^2\Sigma^+$ transition (*12*). The $v'' = 0$ combination differences for the new transition agree well (within the experimental error) to the corresponding values from the $C^2\Pi$–$X^2\Sigma^+$ transition. Although the higher lying electronic states of RuN were not predicted in the previous *ab initio* calculation (*12*), the present observation is consistent with the experimental (*18–20*) and theoretical (*21*) results available for the isovalent RhC molecule. Our new transition of RuN is analogous to the $E^2\Sigma^+$–$X^2\Sigma^+$ transition (revised notation, as discussed below) of RhC.

The rotational assignment in different bands was straight forward by comparing the combination differences for the common vibrational levels, as well as with the ground state combination differences obtained in our previous analysis (*12*). The rotational constants for the individual vibrational levels were determined by fitting the observed line positions to the energy level expression of the $^2\Sigma$ state utilizing the effective Hamiltonian of Brown

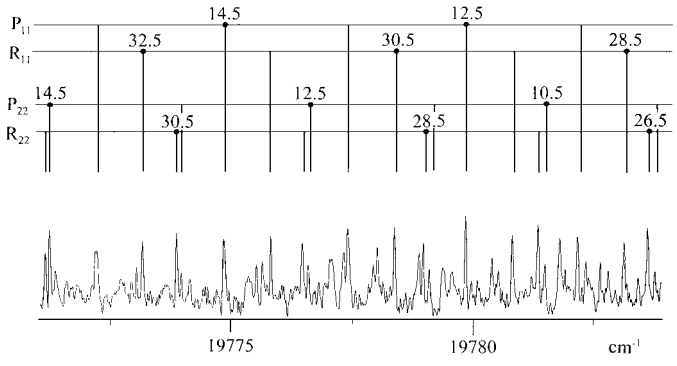

FIG. 1. An expanded portion of the 1–0 band of the $F^2\Sigma^+$–$X^2\Sigma^+$ system with some lines marked in the *R* and *P* branches of ^{102}RuN.

et al. (*23*). The matrix elements for a $^2\Sigma$ Hamiltonian are listed by Douay *et al.* (*24*). The constants T_v, B_v, D_v, γ_v, and γ_{D_v} were determined for the lower $X^2\Sigma^+$ state, while additional higher order constants such as H_v and γ_{H_v} were also required in the excited state in order to minimize the standard deviation of the fit. To constrain the spin splitting in the lower state, lines from the previous work (*12*) were added to the final fit. The rotational lines were given suitable weighting depending on the signal-to-noise ratio and extent of blending. The rotational line positions in the different bands of the new transition are provided in Table 1.

Rotational analysis indicates that all three vibrational levels of the excited state are affected by interactions from a close-lying state (or states). The observed minus calculated difference in the 0–0 and 0–1 bands (Table 1) indicates that the e-parity levels of the $v' = 0$ level are perturbed for $J' \geq 36.5$ and the f-parity levels of the excited state are perturbed at low J values ($J' \leq 16.5$). The high-J e-parity lines after the perturbation could not be identified in the 0–0 and 0–1 bands. The e-parity levels of the 1–0 band are free from perturbation although a small local perturbation has been observed near $J' = 52.5$ for the f-parity levels. In the 2–0 band, the e-parity levels again are not perturbed but the f-levels are affected at $J' \geq 45.5$. A number of rotational lines of both parities in the vicinity of perturbation were given lower weighting. The rotational constants obtained for the different vibrational level of the lower and upper $^2\Sigma^+$ states are provided in Table 2.

DISCUSSION

In our previous work on RuN (*12*), we have assigned a near infrared transition as $C^2\Pi$–$X^2\Sigma^+$. This assignment was supported by our *ab initio* calculations on the spectroscopic properties of the low-lying electronic states of RuN. The rotational analysis of the new visible bands confirms that the new transition has a lower state in common with the $C^2\Pi$–$X^2\Sigma^+$ transition. The ground state of RuN is established as $^2\Sigma^+$ from our *ab initio* calculations (*12*). This state arises from the configuration

$$1\sigma^2 2\sigma^2 1\pi^4 1\delta^4 3\sigma^1 \quad (X^2\Sigma^+). \qquad [1]$$

The promotion of an electron from 1δ to 3σ orbital results in the first excited $^2\Delta$ state arising from the configuration,

$$1\sigma^2 2\sigma^2 1\pi^4 1\delta^3 3\sigma^2 \quad (^2\Delta) \qquad [2]$$

This state has been labeled as the $A^2\Delta$ state (*12*). The next four doublet excited states arise from the promotion of an electron from the 1δ orbital to the 2π orbital,

$$1\sigma^2 2\sigma^2 1\pi^4 1\delta^3 3\sigma^1 2\pi^1 \quad [^2\Pi(2), {}^2\Phi(2)]. \qquad [3]$$

On the basis of our *ab initio* calculations we have labeled the next two excited states as $B^2\Phi$ and $C^2\Pi$ and the next two excited states may be labeled as $D^2\Phi$ and $E^2\Pi$. The next state to higher energy arises from the promotion of an electron from the 3σ orbital to the 4σ orbital, giving rise to a $^2\Sigma^+$ state,

$$1\sigma^2 2\sigma^2 1\pi^4 1\delta^4 4\sigma^1 \quad (^2\Sigma^+). \qquad [4]$$

We label this state as $F^2\Sigma^+$. This state is most probably the excited state of our new electronic transition, the subject of the present paper. Unfortunately this state was not included in our previous *ab initio* calculation but can safely be labeled as $F^2\Sigma^+$ based on the trend in energy levels and the *ab initio* results available for the isovalent RhC by Tan *et al.* (*21*).

It is now well known that the electronic structure of diatomic transition metal nitride molecules is very similar to that of isoelectronic diatomic carbides as discussed in our previous papers on RuN (*12*) and OsN (*13*). For example, IrN (*25–27*) and PtC (*28*), OsN (*13*) and IrC (*29*), and RuN (*12*) and RhC (*18–21*) have very similar electronic structure. Therefore some useful conclusions can be drawn about the new $^2\Sigma^+$ excited state of RuN using the available experimental (*18–20*) and theoretical (*21*) results for RhC. A review of the previous experimental studies of RhC indicates that the four electronic states of RhC initially labeled by Lagerqvist and Scullman (*18*) and Kaving and Scullman (*19*) as $A^2\Pi_r$, $B^2\Sigma^+$, $C^2\Sigma^+$, and $D^2\Sigma^-$ have been relabeled as $B^2\Pi_r$, $D^2\Pi_{3/2}$, $E^2\Sigma^+$, and $D^2\Pi_{1/2}$, respectively, by Balfour *et al.* (*20*) after an extensive investigation of the visible spectrum obtained in a laser ablation–supersonic molecular beam experiment. This revision was supported by a recent *ab initio* study of this molecule by Tan *et al.* (*21*). In the present paper we have decided to use the revised labels of Balfour *et al.* (*20*) to refer to the known electronic states of RhC. The $C^2\Phi$ state of RhC, formally analogous to the $B^2\Phi$ state of RuN, was not mentioned by Balfour *et al.* (*20*). The $C^2\Pi$ state of RuN (*12*) is analogous to the $D^2\Pi$ state of RhC (*20, 21*) and our new $^2\Sigma^+$ state of RuN at 18 866 cm^{-1} is analogous to the $E^2\Sigma^+$ state of RhC (*20, 21*).

Although additional higher-lying $^2\Pi$ excited states of RuN are yet to be observed, some useful conclusions could be drawn from the observed perturbations in the $F^2\Sigma^+$ state and the *ab initio* calculations for RhC by Tan *et al.* (*21*). The $D^2\Pi$ state of RhC (revised notation) has been observed just below the $E^2\Sigma^+$ state, as has been predicted by the *ab initio* calculation of Tan *et al.* (*21*). The $D^2\Pi$ and $E^2\Sigma^+$ states are involved in a strong interaction which results in extensive perturbations in these two states of RhC (*18, 20*). A similar interaction in RuN between a close-lying $^2\Pi$ state and the new $F^2\Sigma^+$ state is presumably responsible for the observed perturbations in the $F^2\Sigma^+$ state, although perturbing $^2\Pi$ state has not been observed yet for RuN. The effect of interactions are clearly visible in the rotational constants of the $F^2\Sigma^+$ state (Table 2). The excited state constants, particularly the distortion and spin-splitting constants in Table 2, vary in an irregular manner compared to those of the ground state. This, as well as the need for higher order constants in the excited state is a reflection of these interactions. The effect of the $^2\Pi$ state is also prominent

TABLE 1
Observed Line Positions (in cm^{-1}) for the $F^2\Sigma^+ - X^2\Sigma^+$ System of ^{102}RuN

J	R_{11}	O-C	P_{11}	O-C	R_{22}	O-C	P_{22}	O-C	J
				0-1					
9.5			17744.650	-0.014					9.5
10.5	17763.577	0.006	17742.673	0.009					10.5
11.5	17763.454	0.000	17740.562	0.001					11.5
12.5	17763.255	0.021	17738.350	-0.003					12.5
13.5	17762.906	-0.001	17736.039	-0.003					13.5
14.5	17762.470	-0.003	17733.626	0.000					14.5
15.5	17761.930	-0.002	17731.104	0.001					15.5
16.5	17761.282	0.000	17728.474	-0.002					16.5
17.5	17760.526	0.002	17725.740	-0.001	17759.895 a	0.702			17.5
18.5	17759.649	-0.005	17722.886	-0.012	17758.793 a	0.567	17720.272 a	0.881	18.5
19.5	17758.672	-0.001	17719.947	0.001	17757.575 a	0.419	17717.031 a	0.699	19.5
20.5	17757.575	-0.004	17716.886	0.002	17756.292 a	0.310	17713.726 a	0.552	20.5
21.5	17756.383	0.013	17713.726	0.015	17754.946 a	0.241	17710.325 a	0.413	21.5
22.5	17755.047	0.003	17710.427	0.001	17753.493 a	0.167	17706.859 a	0.312	22.5
23.5	17753.609	0.009	17707.026	0.000	17751.972 a	0.128	17703.305 a	0.224	23.5
24.5	17752.044	0.008	17703.522	0.012	17750.346 a	0.086	17699.687 a	0.175	24.5
25.5	17750.346	-0.003	17699.885	0.009	17748.632 a	0.060	17695.972 a	0.130	25.5
26.5	17748.498 a	-0.040	17696.123	0.001	17746.828 a	0.046	17692.165 a	0.096	26.5
27.5	17746.524 a	-0.075	17692.238	-0.010	17744.918 a	0.027	17688.259 a	0.065	27.5
28.5	17744.367 a	-0.163	17688.206 a	-0.043	17742.916	0.020	17684.272 a	0.055	28.5
29.5	17742.047 a	-0.282	17684.040 a	-0.083	17740.807	0.007	17680.171 a	0.032	29.5
30.5	17739.550 a	-0.442	17679.704 a	-0.165	17738.600	-0.001	17675.977 a	0.018	30.5
31.5	17736.855 a	-0.660	17675.206 a	-0.276	17736.295	-0.006	17671.688	0.009	31.5
32.5	17733.906 a	-0.991	17670.527 a	-0.433	17733.906	0.007	17667.303	0.006	32.5
33.5	17730.781 a	-1.350	17665.629 a	-0.671	17731.382	-0.012	17662.811	-0.002	33.5
34.5	17727.397 a	-1.819	17660.531 a	-0.968	17728.795	0.005	17658.224	-0.005	34.5
35.5	17723.780 a	-2.367	17655.202 a	-1.351	17726.075	-0.009	17653.537	-0.007	35.5
36.5			17649.633 a	-1.823			17648.756	-0.004	36.5
37.5			17643.863 a	-2.344			17643.863	-0.011	37.5
38.5					17717.357	-0.000	17638.883	-0.006	38.5
39.5					17714.248	0.001	17633.801	-0.002	39.5
40.5					17711.037	0.000	17628.619	0.001	40.5
41.5					17707.724	-0.001	17623.336	0.003	41.5
42.5					17704.316	0.003	17617.947	-0.001	42.5
43.5					17700.785	-0.014	17612.472	0.008	43.5
44.5					17697.185	-0.001	17606.896	0.016	44.5
45.5					17693.475	0.003	17601.196	-0.001	45.5
46.5					17689.658	0.001	17595.420	0.006	46.5
47.5					17685.758	0.017	17589.534	0.001	47.5
48.5							17583.542	-0.010	48.5
49.5					17677.603	-0.003	17577.472	0.001	49.5
50.5							17571.285	-0.004	50.5
51.5					17669.053	-0.011	17565.005	-0.003	51.5
52.5					17664.637	-0.002	17558.626	-0.001	52.5
53.5					17660.110	-0.001	17552.135	-0.010	53.5
54.5					17655.480	0.000			54.5
55.5					17650.747	0.003			55.5
56.5					17645.906	0.003			56.5
				0-0					
7.5	18871.434	0.010	18856.488	0.002					7.5
8.5	18871.563	-0.001	18854.627	-0.009					8.5
9.5	18871.596	0.002	18852.656	-0.020					9.5
10.5	18871.525	0.012	18850.609	0.002					10.5

Note. Lines affected by interactions are marked by "a" and were given lower weights in the fit, see text for details.

TABLE 1—*Continued*

J	R_{11}	O-C	P_{11}	O-C	R_{22}	O-C	P_{22}	O-C	J
11.5	18871.328	0.007	18848.421	-0.005					11.5
12.5	18871.019	0.003	18846.141	0.004					12.5
13.5	18870.594	-0.005	18843.739	0.004	18871.103 a	1.467			13.5
14.5	18870.076	0.007	18841.224	0.002	18870.246 a	1.269			14.5
15.5	18869.430	0.005	18838.590	-0.006	18869.279 a	1.071			15.5
16.5	18868.663	-0.002	18835.855	-0.003	18868.208 a	0.879			16.5
17.5	18867.786	-0.003	18833.004	-0.002	18867.047 a	0.706			17.5
18.5	18866.795	0.000	18830.039	0.001	18865.801 a	0.559	18827.326 a	0.919	18.5
19.5	18865.682	0.000	18826.956	-0.000	18864.452 a	0.419	18823.918 a	0.706	19.5
20.5	18864.452	0.003	18823.749	-0.006	18863.032 a	0.317	18820.468 a	0.561	20.5
21.5	18863.098	0.003	18820.436	-0.002	18861.529 a	0.242	18816.910 a	0.416	21.5
22.5	18861.616	-0.002	18817.003	0.004	18859.931 a	0.182	18813.288 a	0.317	22.5
23.5	18860.013	-0.002	18813.449	0.008	18858.230 a	0.129	18809.576 a	0.237	23.5
24.5	18858.277	-0.008	18809.766	0.007			18805.773 a	0.177	24.5
25.5	18856.405 a	-0.020	18805.965	0.013	18854.548 a	0.071	18801.881 a	0.135	25.5
26.5	18854.387 a	-0.047	18802.016	-0.003	18852.550 a	0.050	18797.884 a	0.097	26.5
27.5	18852.216 a	-0.092	18797.943 a	-0.015	18850.444 a	0.029	18793.795 a	0.076	27.5
28.5	18849.877 a	-0.170	18793.718 a	-0.047	18848.237 a	0.017	18789.592 a	0.051	28.5
29.5	18847.350 a	-0.294	18789.340 a	-0.099	18845.925	0.009	18785.293 a	0.038	29.5
30.5	18844.650 a	-0.450	18784.805 a	-0.172	18843.505	0.003	18780.880 a	0.020	30.5
31.5	18841.731 a	-0.678	18780.091 a	-0.285	18840.977	-0.003	18776.368	0.010	31.5
32.5	18838.590 a	-0.979	18775.190 a	-0.443	18838.344	-0.006	18771.747	-0.001	32.5
33.5	18835.209 a	-1.367	18770.069 a	-0.675	18835.605	-0.005	18767.030	0.001	33.5
34.5	18831.606 a	-1.819	18764.724 a	-0.984	18832.758	-0.004	18762.202	-0.000	34.5
35.5	18827.749 a	-2.364	18759.155 a	-1.364			18757.269	0.001	35.5
36.5			18753.345 a	-1.828	18826.737	-0.006	18752.226	0.000	36.5
37.5			18747.294 a	-2.373	18823.574	0.004	18747.066	-0.011	37.5
38.5					18820.285	-0.005	18741.818	-0.003	38.5
39.5					18816.910	0.008			39.5
40.5					18813.403	-0.002	18730.984	-0.003	40.5
41.5					18809.806	0.003	18725.416	0.006	41.5
42.5					18806.101	0.010	18719.733	0.007	42.5
43.5					18802.278	0.006	18713.943	0.006	43.5
44.5					18798.343	-0.002	18708.035	-0.004	44.5
45.5					18794.322	0.011	18702.033	-0.004	45.5
46.5					18790.173	0.004	18695.928	0.001	46.5
47.5					18785.920	0.002	18689.721	0.011	47.5
48.5					18781.557	-0.003	18683.385	-0.002	48.5
49.5					18777.089	-0.003	18676.957	0.000	49.5
50.5					18772.497	-0.020	18670.408	-0.012	50.5
51.5					18767.824	-0.008	18663.779	0.002	51.5
52.5					18763.041	0.004	18657.026	0.001	52.5
53.5					18758.123	-0.009	18650.163	-0.003	53.5
54.5					18753.121	0.005	18643.188	-0.011	54.5
55.5					18748.004 a	0.016	18636.119	-0.004	55.5
56.5					18742.784 a	0.035	18628.939	0.002	56.5
57.5							18621.666 a	0.025	57.5
				1-0					
3.5							19795.125	0.000	3.5
4.5			19795.405	0.019			19793.525	-0.004	4.5
5.5			19793.866	0.014			19791.814	-0.003	5.5
6.5			19792.198	-0.003			19789.999	0.008	6.5
7.5			19790.438	0.002			19788.051	0.002	7.5
8.5			19788.561	0.005	19804.789	0.000	19785.990	-0.002	8.5

TABLE 1—*Continued*

J	R_{11}	O-C	P_{11}	O-C	R_{22}	O-C	P_{22}	O-C	J
9.5	19805.399	0.005	19786.564	0.002	19804.591	-0.006	19783.825	0.006	9.5
10.5	19805.252	-0.011	19784.442	-0.010	19804.294	0.004	19781.537	0.004	10.5
11.5	19805.015	-0.002	19782.216	-0.011	19803.862	-0.004	19779.134	0.003	11.5
12.5	19804.656	0.000	19779.882	-0.004	19803.332	0.003	19776.617	0.003	12.5
13.5	19804.175	-0.005	19777.441	0.010	19802.675	-0.001	19773.984	0.001	13.5
14.5	19803.586	-0.002	19774.867	0.006	19801.907	0.001	19771.234	-0.002	14.5
15.5	19802.874	-0.007	19772.178	0.002	19801.034	0.012	19768.374	-0.001	15.5
16.5	19802.062	0.005	19769.370	-0.006	19800.022	-0.001	19765.403	0.005	16.5
17.5	19801.116	-0.003	19766.460	-0.001	19798.905	-0.003	19762.308	0.001	17.5
18.5	19800.062	-0.004	19763.432	-0.000	19797.678	0.001	19759.105	0.005	18.5
19.5	19798.905	0.008	19760.296	0.009	19796.331	0.000	19755.772	-0.007	19.5
20.5	19797.611	-0.001	19757.022	-0.004	19794.870	0.001	19752.346	0.004	20.5
21.5	19796.212	0.000	19753.647	-0.004	19793.292	0.001	19748.790	0.000	21.5
22.5	19794.696	-0.000	19750.164	0.002	19791.601	0.003	19745.126	0.002	22.5
23.5	19793.066	0.001	19746.559	0.002	19789.787	-0.002	19741.347	0.005	23.5
24.5	19791.321	0.003	19742.842	0.005	19787.864	-0.000	19737.445	-0.001	24.5
25.5			19739.004	0.002	19785.822	-0.002	19733.437	0.003	25.5
26.5	19787.476	0.000	19735.054	0.002	19783.666	-0.001	19729.305	-0.002	26.5
27.5	19785.383	0.002	19730.990	0.003	19781.392	-0.003	19725.064	-0.001	27.5
28.5	19783.171	0.000	19726.808	0.001	19779.007	-0.000	19720.708	-0.001	28.5
29.5	19780.846	0.000	19722.511	-0.001	19776.496	-0.007	19716.236	0.000	29.5
30.5	19778.406	0.002	19718.101	-0.001	19773.888	0.005	19711.646	-0.002	30.5
31.5	19775.844	-0.002	19713.579	0.002	19771.146	-0.001	19706.945	-0.001	31.5
32.5	19773.173	-0.001	19708.944	0.007	19768.293	-0.001	19702.126	-0.002	32.5
33.5	19770.380	-0.004	19704.184	0.002	19765.322	-0.004	19697.190	-0.005	33.5
34.5	19767.467	-0.011	19699.316	0.005	19762.240	-0.000	19692.153	0.006	34.5
35.5	19764.463	0.006	19694.331	0.004	19759.025	-0.014	19686.983	-0.000	35.5
36.5	19761.317	-0.003	19689.222	-0.005	19755.718	-0.003			36.5
37.5	19758.070	0.004	19684.012	0.001	19752.284	-0.003	19676.309	-0.000	37.5
38.5	19754.693	-0.004	19678.678	-0.003	19748.741	0.005	19670.800	0.000	38.5
39.5	19751.212	0.001	19673.234	-0.001	19745.064	-0.003	19665.173	-0.001	39.5
40.5	19747.607	-0.002	19667.674	-0.001	19741.288	0.004	19659.432	-0.001	40.5
41.5	19743.892	0.002	19661.995	-0.004	19737.386	0.004	19653.577	0.001	41.5
42.5	19740.053	-0.003	19656.214	0.006	19733.365	0.002	19647.598	-0.005	42.5
43.5	19736.106	0.000	19650.300	-0.003	19729.224	-0.004	19641.518	0.002	43.5
44.5	19732.032	-0.006	19644.280	-0.001	19724.982	0.006	19635.310	-0.002	44.5
45.5	19727.855	-0.000	19638.146	0.000	19720.612	0.006	19629.000	0.008	45.5
46.5	19723.555	-0.001	19631.898	0.004	19716.125	0.006	19622.553	-0.003	46.5
47.5	19719.144	0.005	19625.524	-0.003	19711.519	0.004	19616.009	0.005	47.5
48.5	19714.615	0.009	19619.047	0.001			19609.340	0.003	48.5
49.5	19709.953	-0.005	19612.449	0.000	19701.949	-0.004	19602.566	0.013	49.5
50.5	19705.194	0.002	19605.735	-0.002	19696.990 a	-0.006	19595.641	-0.012	50.5
51.5	19700.320	0.011	19598.907	-0.003	19691.893 a	-0.027	19588.628	-0.008	51.5
52.5			19591.965	-0.002			19581.483 a	-0.021	52.5
53.5	19690.193	-0.001	19584.906	-0.003	19681.488 a	0.072	19574.226 a	-0.029	53.5
54.5	19684.966	0.004	19577.738	0.001	19676.026 a	0.040			54.5
55.5	19679.623	0.011	19570.451	0.002	19670.460 a	0.022	19559.483 a	0.076	55.5
56.5	19674.148	0.001	19563.041	-0.004	19664.796 a	0.024	19551.841 a	0.034	56.5
57.5	19668.568	0.004	19555.539	0.013	19658.996	0.010	19544.109 a	0.018	57.5
58.5	19662.849	-0.014	19547.889	-0.003	19653.068	-0.015	19536.281 a	0.023	58.5
59.5	19657.058	0.012	19540.141	-0.001			19528.304	-0.003	59.5
60.5	19651.104	-0.008	19532.286	0.008			19520.246	0.006	60.5
61.5	19645.063	0.001	19524.301	0.004			19512.039	-0.016	61.5
62.5	19638.891	-0.002							62.5
63.5	19632.599	-0.010							63.5

TABLE 1—*Continued*

J	R_{11}	O-C	P_{11}	O-C	R_{22}	O-C	P_{22}	O-C	J
					2-0				
3.5			20717.952	0.005			20716.215	-0.004	3.5
4.5			20716.521	0.013			20714.584	-0.005	4.5
5.5			20714.953	0.005			20712.832	-0.002	5.5
6.5			20713.268	0.005			20710.944	-0.015	6.5
7.5			20711.461	0.003	20725.640	0.001	20708.952	-0.007	7.5
8.5			20709.530	0.001	20725.476	-0.005	20706.832	-0.005	8.5
9.5	20726.177	0.002	20707.475	-0.003	20725.192	-0.009	20704.586	-0.007	9.5
10.5	20725.971	0.005	20705.311	0.007	20724.783	-0.013	20702.213	-0.012	10.5
11.5	20725.640	0.006	20703.014	0.006	20724.259	-0.011	20699.730	-0.005	11.5
12.5	20725.192	0.012	20700.589	-0.001	20723.600	-0.019	20697.128	0.006	12.5
13.5	20724.607	0.004	20698.052	0.004	20722.847	0.002	20694.388	0.003	13.5
14.5	20723.904	0.001	20695.373	-0.012	20721.950	0.002	20691.521	-0.006	14.5
15.5	20723.091	0.012	20692.605	0.006	20720.931	0.003			15.5
16.5	20722.133	-0.001	20689.687	-0.004	20719.794	0.010			16.5
17.5	20721.054	-0.011	20686.658	-0.003	20718.520	0.003	20682.220	0.008	17.5
18.5	20719.874	0.001	20683.504	-0.004	20717.120	-0.006	20678.862	-0.000	18.5
19.5	20718.561	0.003	20680.232	0.000	20715.605	-0.007	20675.403	0.014	19.5
20.5	20717.120	-0.001	20676.826	-0.008	20713.972	-0.002	20671.784	-0.007	20.5
21.5	20715.554	-0.006	20673.311	-0.002	20712.210	0.000	20668.083	0.011	21.5
22.5	20713.874	-0.002	20669.673	0.002	20710.337	0.012	20664.235	0.006	22.5
23.5	20712.060	-0.009	20665.903	-0.002	20708.319	0.005	20660.270	0.008	23.5
24.5	20710.143	0.004	20662.013	-0.004	20706.179	-0.001	20656.172	-0.001	24.5
25.5	20708.073	-0.013	20658.005	-0.002	20703.922	-0.000	20651.967	0.008	25.5
26.5			20653.864	-0.010	20701.544	0.005	20647.632	0.009	26.5
27.5			20649.616	-0.002	20699.039	0.006	20643.160	-0.003	27.5
28.5	20701.200	0.013	20645.235	-0.006	20696.406	0.004	20638.580	0.000	28.5
29.5	20698.646	0.005	20640.746	0.006	20693.646	0.000	20633.872	-0.001	29.5
30.5	20695.970	0.000	20636.130	0.013	20690.757	-0.008	20629.045	0.003	30.5
31.5	20693.181	0.005	20631.380	0.009	20687.750	-0.010	20624.085	-0.003	31.5
32.5	20690.259	0.000	20626.514	0.011	20684.604 a	-0.027	20619.006	-0.005	32.5
33.5	20687.219	0.000	20621.508	-0.004	20681.346 a	-0.030	20613.807	-0.002	33.5
34.5	20684.052	-0.002	20616.404	0.005	20677.958 a	-0.039	20608.462 a	-0.021	34.5
35.5	20680.767	0.001	20611.155	-0.006	20674.438 a	-0.055	20603.010 a	-0.024	35.5
36.5	20677.347	-0.006	20605.803	0.000	20670.781 a	-0.082	20597.419 a	-0.041	36.5
37.5	20673.812	-0.006	20600.320	0.000	20667.010 a	-0.097	20591.705 a	-0.058	37.5
38.5	20670.149	-0.008	20594.714	-0.001	20663.103 a	-0.124	20585.864 a	-0.076	38.5
39.5	20666.373	-0.001	20588.986	0.000	20659.048 a	-0.174	20579.897 a	-0.097	39.5
40.5	20662.467	0.002	20583.130	-0.006	20654.872 a	-0.218	20573.791 a	-0.133	40.5
41.5	20658.438	0.005	20577.163	0.001	20650.538 a	-0.295	20567.562 a	-0.167	41.5
42.5	20654.285	0.009	20571.070	0.005	20646.074 a	-0.376	20561.187 a	-0.223	42.5
43.5	20649.990	-0.005	20564.842	-0.003	20641.427 a	-0.514	20554.655 a	-0.312	43.5
44.5	20645.587	-0.003	20558.508	0.007	20636.618 a	-0.688	20548.022 a	-0.376	44.5
45.5	20641.063	0.003	20552.032	-0.003			20541.185 a	-0.520	45.5
46.5	20636.411	0.006	20545.446	0.001			20534.196 a	-0.691	46.5
47.5	20631.621	-0.004	20538.730	-0.001					47.5
48.5	20626.717	-0.004	20531.900	0.005					48.5
49.5	20621.687	-0.005	20524.937	0.002					49.5
50.5	20616.543	0.005	20517.860	0.009					50.5
51.5	20611.250	-0.008	20510.646	0.001					51.5
52.5	20605.857	0.003							52.5
53.5	20600.320	-0.004							53.5

TABLE 2
Molecular Constants[a] (in cm^{-1}) for the $F^2\Sigma^+$–$X^2\Sigma^+$ System of ^{102}RuN

	$X^2\Sigma^+$		$F^2\Sigma^+$		
Constants	v=0	v=1	v=0	v=1	v=2
T_v	0.0	1108.3235(22)	18866.3825(26)	19800.38387(67)	20721.53954(62)
B_v	0.5527789(30)	0.5493321(49)	0.4984529(78)	0.4952342(35)	0.4914497(34)
$10^6 \times D_v$	0.55115(39)	0.55807(99)	1.5349(76)	0.5875(13)	0.6332(11)
$10^{10} \times H_v$	–	--	-2.336(41)	-0.0121(24)	--
$10^2 \times \gamma_v$	-4.4415(18)	-4.487(11)	-0.996(46)	1.7430(58)	2.5314(81)
$10^6 \times \gamma_{Dv}$	-0.2097(45)	--	-1.14(99)	-0.761(60)	5.331(93)
$10^8 \times \gamma_{Hv}$	–	--	-5.893(75)	0.0482(14)	--
	--	--	--	--	--

[a] Numbers in parentheses are one standard deviation in the last digits quoted.

in the spin splitting constants, which have the values of $\gamma_0 = -0.996(46) \times 10^{-2}$ cm^{-1}, $\gamma_1 = 1.7430(58) \times 10^{-2}$ cm^{-1}, and $\gamma_2 = 2.5314(81) \times 10^{-2}$ cm^{-1} in the $F^2\Sigma^+$ state.

In a private communication, Liévin (*30*) informed us of some exploratory CASSCF calculations on the doublet states of RuN around 18 000 cm^{-1} which he performed at the time of our previous work on the $C^2\Pi$–$X^2\Sigma^+$ transition of RuN (*12*). At that time MRCI calculations were not performed for the higher lying states because we were concerned with only the low-lying electronic states. The previous CASSCF calculations are very instructive. As a result of our work on the new $^2\Sigma^+$ state Liévin (*30*) has also performed MRCI calculations at a distance of 1.6 Å on the $2\,^2\Sigma^+$ and the 2 and $3\,^2\Pi$ states of RuN in order to check the assigned configurations and energies. In order to include the $3\,^2\Pi$ state in the calculations, the following additional configuration was also considered:

$$1\sigma^2 2\sigma^2 1\pi^4 1\delta^4 2\pi^1 \quad (3^2\Pi). \qquad [5]$$

The wave function of the $3\,^2\Pi$ state corresponds to a mixing between configurations [3] and [5] with a large weight on configuration [5]. In this calculation the $2\,^2\Pi$ ($E^2\Pi$) is predicted to lie below 15 000 cm^{-1} and the $3\,^2\Pi$ state is predicted to lie near 18 000 cm^{-1}. These calculations also predict that the $2\,^2\Sigma^+$ state arising from the configuration $1\sigma^2 2\sigma^2 1\pi^4 1\delta^4 4\sigma^1$ lies at 18 600 cm^{-1} which confirms our assignment of the new $2\,^2\Sigma^+$ state. Originally we thought that the observed perturbations in the new $^2\Sigma^+$ state were caused by the $2\,^2\Pi$ ($E^2\Pi$) state. On that basis we labeled the new $^2\Sigma^+$ state as $F^2\Sigma^+$. But the recent work of Liévin (*30*) suggests that the $3\,^2\Pi$ state may be a better candidate for the perturbing state rather than the $2\,^2\Pi$ ($E^2\Pi$) state. It was also found that adding the third $^2\Pi$ state in the calculation induces a larger configuration mixing in the two lowest $^2\Pi$ states than was predicted in our previous paper (*12*) (but the energies do not change by much). This was explained by Liévin as showing that the configurations [3] and [5] are close in energy, with configuration [3] being more stable than configuration [5]. The $1\,^2\Pi$ ($C^2\Pi$) state is richer in configuration [3] and the $2\,^2\Pi$ ($E^2\Pi$) and $3\,^2\Pi$ states are mixtures of configurations [3] and [5]. Some preliminary calculation were also performed on RhC and the switch in energy order of configurations [3] and [5] with respect to RuN was confirmed.

The rotational constants for the individual vibrational levels (Table 2) have been used to evaluate the equilibrium molecular constants (Table 3). Because only $v = 0$ and 1 vibrational levels have been observed in the ground state, the equilibrium constants for this state were determined from an exact fit, providing $\Delta G(1/2) = 1108.3235(22)$ cm^{-1}, $B_e = 0.554\,502\,3(42)$ cm^{-1}, and $\alpha_e = 0.003\,446\,8(57)$ cm^{-1}. The uncertainties quoted in parentheses were derived from the propagation of errors but the actual uncertainties may be larger than the quoted values. It is noted that the gas phase ground state vibrational interval [1108.3235(22) cm^{-1}] is considerably higher than the value (981.5 cm^{-1}) obtained by Citra and Andrews (*16*) in their laser-ablation matrix experiment. The T_0, T_1, and T_2 values for the $F^2\Sigma^+$ state (Table 2) provide $\omega_e = 946.8471(40)$ cm^{-1}, $\omega_e x_e = 6.4229(14)$ cm^{-1} for the $F^2\Sigma^+$ state. Note that the excited state rotational constants of Table 2, although well determined, show a rather large deviation

TABLE 3
Equilibrium Constants[a] (in cm^{-1}) for the $X^2\Sigma^+$ and $F^2\Sigma^+$ States of ^{102}RuN

Constants	$X^2\Sigma^+$	$F^2\Sigma^+$
ω_e	[1108.3235(22)][b]	946.8471(40)
$\omega_e x_e$	–	6.4229(14)
B_e	0.5545023(42)	0.50085(21)
α_e	0.0034468(57)	0.00375(10)
r_e(Å)	1.5714269(60)	1.65345(34)

[a] Values in parentheses are one standard deviation in the last digits quoted.
[b] $\Delta G(1/2)$ value.

from the expected trend. For example, the experimental values of $B_0-B_1 = 0.003\,218\,7$ cm^{-1} and $B_1-B_2 = 0.003\,784\,5$ cm^{-1} have a large difference contrary to expectation. Part of the reason is the presence of perturbations in the $v' = 0$ vibrational level at very low J values (e-levels at $J' \geq 36.5$ and f-levels at $J' \leq 16.5$). As can be seen in from the observed minus calculated values in Table 1, the f-parity lines are perturbed at lower J values. Such a parity-dependent interaction is consistent with a perturbation by a $^2\Pi_{1/2}$ state with a large Λ-doubling splitting. Because of this perturbation the B_0 value may be in error by a larger amount than determined from the fit. We have, therefore, given lower weighting to the B_0 value of the excited state while determining the equilibrium rotational constants for the excited state. The equilibrium constants determined in this manner are $B_e = 0.50085(21)$ cm^{-1} and $\alpha_e = 0.00375(10)$ cm^{-1}. The equilibrium rotational constants have been used to evaluate the equilibrium bond lengths. The values of $r''_e = 1.5714269(60)$ Å and $r'_e = 1.65345(34)$ Å have been determined for the ground and the excited states of RuN. The equilibrium constants have been provided in Table 3. The equilibrium ground state bond length of $r''_e = 1.5714269(60)$ Å compares well with the predicted value of $r''_e = 1.578$ Å from the previous *ab initio* calculation (*12*). This value can also be compared with the values of $r''_e = 1.716$ Å for RuO (*31*), $r''_e = 1.613$ Å for RhC (*19*), $r''_0 = 1.581$ Å for FeN (*11*), and $r''_e = 1.618$ Å OsN (*13*). The short bond length of RuN compared to that of RuO is consistent with a formal triple bond between the atoms.

CONCLUSION

The high-resolution spectrum of RuN has been observed in the region 12 000–35 000 cm^{-1} using a Fourier transform spectrometer. The new bands observed in the region 17 500–22 000 cm^{-1} have been assigned to a new $^2\Sigma^+$–$^2\Sigma^+$transition with its 0–0 band near 18 866.4 cm^{-1}. This transition has the ground state of RuN as its lower state and has been labeled as $F^2\Sigma^+$–$X^2\Sigma^+$, analogous to the $E^2\Sigma^+$–$X^2\Sigma^+$ transition of isovalent RhC (*20*). The molecular parameters for both the states have been derived on the basis of a rotational analysis of the 0–1, 0–0, 1–0, and 2–0 bands. The $F^2\Sigma^+$ state is affected by interactions from a close-lying $^2\Pi$ state as has been observed for the $E^2\Sigma^+$ state of RhC (*20*). The ground state equilibrium bond length of $r''_e = 1.5714$ Å for RuN is similar to the values of $r''_0 = 1.580$ Å for FeN (*11*) and $r''_e = 1.6180$ Å for OsN (*13*).

ACKNOWLEDGMENTS

We thank M. Dulick, C. Plymate, and D. Branston of the National Solar Observatory for assistance in obtaining the spectra. The Kitt Peak National Observatory and the National Solar Observatory are operated by the Association of Universities for Research in Astronomy, Inc., under contract with the National Science Foundation. The research described here was supported by funding from the NASA laboratory astrophysics program. Some support was also provided by the Natural Sciences and Engineering Research Council of Canada. We also thank J. Liévin for his comments on this paper and suggestions based on his unpublished work on the excited states of the RuN molecule.

REFERENCES

1. C. W. Bauschlicher, Jr., S. P. Walch, and S. R. Langhoff, *in* "Quantum Chemistry: The Challenge of Transition Metals in Coordination Chemistry" (A. Veillard, Ed.), NATO ASI Series. Reidel, Dordrecht, 1986.
2. F. A. Cotton, G. Wilkinson, C. A. Murillo, and M. Bochmann, "Advanced Inorganic Chemistry, A Comprehensive Text," 6th ed. Wiley, New York, 1999.
3. M. Grunze, *in* "The Chemical Physics of Solid Surfaces and Heterogeneous Catalysis" (D. A. King and D. P. Woodruff, Eds.), Vol. 4, p. 143. Elsevier, New York, 1982.
4. F. Gassner, E. Dinjus, and W. Leitner, *Organometallics* **15,** 2078–2082 (1996).
5. Y. Yerle, *Astron. Astrophys*. **73,** 346–351 (1979).
6. D. L. Lambert and R. E. S. Clegg, *Mon. Not. R. Astron. Soc*. **191,** 367–389 (1980).
7. B. Lindgren and G. Olofsson, *Astron. Astrophys*. **84,** 300–303 (1980).
8. O. Engvold, H. Wöhl, and J. W. Brault, *Astron. Astrophys. Suppl. Ser*. **42,** 209–212 (1980).
9. R. S. Ram, P. F. Bernath, and L. Wallace, *Astrophys. J. Suppl Ser*. **107,** 443–449 (1996).
10. R. S. Ram and P. F. Bernath, *J. Mol. Spectrosc*. **184,** 401–412 (1997), and references therein.
11. K. Aiuchi and K. Shibuya, *J. Mol. Spectrosc*. **204,** 235–261 (2000).
12. R. S. Ram, J. Liévin, and P. F. Bernath, *J. Chem. Phys*. **109,** 6329–6337 (1998).
13. R. S. Ram, J. Liévin, and P. F. Bernath, *J. Chem. Phys.* **111,** 3449–3456 (1999).
14. A. Fiedler and S. Iwata, *Chem. Phys. Lett*. **271,** 143–151 (1997).
15. M. R. A. Blomberg and P. E. M. Siegbahn, *Theor. Chim. Acta* **81,** 365–374 (1992).
16. A. Citra and L. Andrews, *J. Am. Chem. Soc.* **121,** 11 567–11 568 (1999); *J. Phys. Chem*. **104,** 1152–1161 (2000).
17. J. Häglund, A. F. Guillermet, G. Grimvall, and M. Körling, *Phys. Rev. B* **48,** 11 685–11 691 (1993).
18. A. Lagerqvist and R. Scullman, *Ark. Fys.* **32,** 479–508 (1966).
19. B. Kaving and R. Scullman, *J. Mol. Spectrosc*. **32,** 475–500 (1969).
20. W. J. Balfour, G. S. Fougère, R. F. Hueff, C. X. W. Qian, and C. Zhou, *J. Mol. Spectrosc*. **198,** 393–407 (1999).
21. H. Tan, M. Liao, and K. Balasubramanian, *Chem. Phys. Lett*. **280,** 423–429 (1997).
22. B. A. Palmer and R. Engleman, "Atlas of the Thorium Spectrum." Los Alamos National Laboratory, Los Alamos, 1983.
23. J. M. Brown, E. A. Colbourn, J. K. G. Watson, and F. D. Wayne, *J. Mol. Spectrosc*. **74,** 294–318 (1979).
24. M. Douay, S. A. Rogers, and P. F. Bernath, *Mol. Phys*. **64,** 425–436 (1988).
25. A. J. Marr, M. E. Flores, and T. C. Steimle, *J. Chem. Phys*. **104,** 8183–8196 (1996).
26. R. S. Ram and P. F. Bernath, *J. Mol. Spectrosc*. **193,** 363–375 (1999).
27. R. S. Ram, J. Liévin, and P. F. Bernath, *J. Mol. Spectrosc.* **197,** 133–146 (1999).
28. T. C. Steimle, K. Y. Jung, and B.-Z. Li, *J. Chem. Phys.* **102,** 5937–5941 (1995).
29. K. Jansson and R. Scullman, *J. Mol. Spectrosc*. **36,** 248–267 (1970).
30. J. Liévin, personal communication.
31. R. Scullman and B. Thelin, *J. Mol. Spectrosc*. **56,** 64–75 (1975).